Journal of Hazardous Materials 188 (2011) 369–374

Contents lists available at ScienceDirect

Journal of Hazardous Materials

journal homepage: www.elsevier.com/locate/jhazmat

Initial fuel temperature effects on burning rate of pool fire

Bing Chen[a], Shou-Xiang Lu[a,*], Chang-Hai Li[a], Quan-Sheng Kang[a,b], Vivien Lecoustre[c]

[a] State Key Laboratory of Fire Science, University of Science and Technology of China, Hefei, Anhui 230027, China
[b] Zhejiang University of Technology, Hangzhou, Zhejiang 310014, China
[c] Department of Fire Protection Engineering, University of Maryland, College Park, MD 20742, USA

ARTICLE INFO

Article history:
Received 21 May 2010
Received in revised form 17 January 2011
Accepted 30 January 2011
Available online 4 February 2011

Keywords:
Pool fire
Burning rate
Temperature distribution
Initial fuel temperature

ABSTRACT

The influence of the initial fuel temperature on the burning behavior of n-heptane pool fire was experimentally studied at the State Key Laboratory of Fire Science (SKLFS) large test hall. Circular pool fires with diameters of 100 mm, 141 mm, and 200 mm were considered with initial fuel temperatures ranging from 290 K to 363 K. Burning rate and temperature distributions in fuel and vessel wall were recorded during the combustion. The burning rate exhibited five typical stages: initial development, steady burning, transition, bulk boiling burning, and decay. The burning rate during the steady burning stage was observed to be relatively independent of the initial fuel temperature. In contrast, the burning rate of the bulk boiling burning stage increases with increased initial fuel temperature. It was also observed that increased initial fuel temperature decreases the duration of steady burning stage. When the initial temperature approaches the boiling point, the steady burning stage nearly disappears and the burning rate moves directly from the initial development stage to the transition stage. The fuel surface temperature increases to its boiling point at the steady burning stage, shortly after ignition, and the bulk liquid reaches boiling temperature at the bulk boiling burning stage. No distinguished cold zone is formed in the fuel bed. However, boiling zone is observed and the thickness increases to its maximum value when the bulk boiling phenomena occurs.

1. Introduction

Pool fires are frequently involved in fire accidents [1]. The pool fire burning rate is uttermost information when predicting the relative hazard of such fire. Its unawareness hinders the evaluation of fire behavior and exact prediction of fire effects.

The burning characteristics of liquid pool fires have been studied in detail during the past decades. Experiments were conducted to measure pool fire burning rate for different fuels and pool diameters. The work of Blinov and Khudiakov [2,3] and Burgess et al. [4] showed that the burning rate of single-component fuels varies with the pool diameter before reaching their asymptotic value when the diameter reaches a critical value, typically of the order of the meter m for most common fuel.

Hayasaka [5] studied the burning rate of non-replenishing small pool fires. It was observed that the fuel temperature influences the burning rate and the reason for various burning rate changes is the difference in the evaporation heat of fuel. Other effects such as wind and boilover phenomena can greatly change a pool's burning rate. Increased wind speed has been shown to decrease the burning rate of aviation fuel, as reported by Apter et al. [6]. But wind and size effects on pool fire may be more complex than indicated by Apter et al. Boilover can occur for certain grades of petroleum crude and for petroleum products that are contaminated with moisture. Boilover typically involves the violent boiling of water, which is relatively at a shallow depth, as the heat from the conductive container and liquid fuel heats the water to boiling. This phenomenon can increase the burning rate by a factor of two or more [7–9]. Finally, experiments have shown the nearly proportionality of the pool fire burning rate on atmospheric pressure [10,11], along with the effects of ventilation in enclosure pool fire [12–14].

Predicting burning rate models have been developed. Considering a quasi-steady assumption, the burning rate of a deep pool is simply expressed as the ratio of the net heat transfer to the fuel surface and the fuel heat of gasification. A global model, presented by Hamins et al. [15], predicts the burning rate of pool fires in quiescent environments. Its predicted values for many fuels are within a factor of two from measured burning rates. Heat transfer and heat balance models in the fuel had been reported by Nakakuki [16,17], along with the heat transfer mechanisms in pool fires. Nakakuki also analyzed the heat transfer between the fuel and the surrounding, focusing on the radiative heat from the flame to the fuel surface and the convective heat from the wall to fuel. Muñoz et al. [18,19] studied the radiative characteristics of large gasoline and diesel pool fires. The maximum burning rates obtained were higher than

* Corresponding author. Tel.: +86 551 3603141; fax: +86 551 3603449.
E-mail address: sxlu@ustc.edu.cn (S.-X. Lu).

0304-3894/$ – see front matter © 2011 Elsevier B.V. All rights reserved.
doi:10.1016/j.jhazmat.2011.01.122

Table 1
Properties of fuel and vessel wall.

Fuel	Density ($g\,cm^{-3}$)	Boiling point (K)	Specific heat (at 293 K) ($J\,mol^{-1}\,K^{-1}$)	Heat of vaporization ($kJ\,mol^{-1}$)	Thermal conductivity (at 293 K) ($W\,m^{-1}\,K^{-1}$)
n-Heptane	0.684	371.6	162.2	31.77	0.13
Steel (300M)	7.830	–	480	–	21

Table 2
Experimental data of burning time and average burning rate of heptane tests.

Test Number No.	Pool diameter D (mm)	Initial fuel temperature $T_{f,0}$ (K)	Duration of stage (2) t_1 (s)	Burning rate of stage (2) $\dot{m}''_2$ ($kg\,m^{-2}\,s^{-1}$)	Duration of stage (4) t_2 (s)	Burning rate of stage (4) $\dot{m}''_4$ ($kg\,m^{-2}\,s^{-1}$)	Burning time t (s)	Average burning rate $\dot{m}''_a$ ($kg\,m^{-2}\,s^{-1}$)
1	100	290	210	0.0073	175	0.018	735	0.012
2	100	319	168	0.0074	224	0.019	674	0.013
3	100	343	92	0.0076	185	0.029	467	0.019
4	100	365	0	–	150	0.044	249	0.034
5	141	290	226	0.012	135	0.022	580	0.015
6	141	319	136	0.013	170	0.025	488	0.018
7	141	343	46	0.013	144	0.043	283	0.03
8	141	365	0	–	112	0.046	235	0.039
9	200	290	200	0.015	144	0.024	530	0.017
10	200	319	125	0.015	112	0.028	459	0.02
11	200	343	87	0.016	71	0.046	274	0.033
12	200	365	0	–	129	0.054	198	0.046

the previously published data. Fay [20] published a model of convective heat transfer between the combustion zone and the liquid fuel pool that provides mass evaporation rates in both adiabatic and non-adiabatic fires

Despite the abundant work on pool fires, it remains a lack of quantitative information on the effects of initial fuel temperatures on pool fire burning rate. This effect was only briefly described by Burgess et al. [4] considering ethyl, ether, methanol, and 95% ethanol burning in a 7.5 cm diameter brine-jacketed burner. The steady burning rate increased when the fuel temperature was raised from −40 °C to 40 °C. Far from being peculiar, pool fire with high initial fuel temperature can occur from leaking operating machines or from fuel storage in a high temperature environment. From a fire prevention and fire defense stance, it is crucial to understand the burning process of pool fire with initial high fuel temperatures.

The aim of this work is to investigate pool fires with different initial fuel temperatures. Pool fire of n-heptane with different diameters and different initial temperatures were conducted indoors to eliminate possible changes in test conditions. Special attention is carried on the effect of fuel initial temperature on burning rate behavior. Measurements of temperature distribution in fuel and vessel wall are also provided. While the aim of this work is to report measured experimental quantities, a brief analysis is provided to discuss the process of burning rate.

2. Experimental

Free burning fires were performed in a large test hall (12 m × 12 m × 12 m) of the State Key Laboratory of Fire Science (SKLFS), China. During the test, the doors and windows were closed, but not sealed. The presence of the room walls and airflow restrictions did not influence significantly the burning behavior of fires because the fire was relative small in size.

Three circular steel trays with the same height of 40 mm but with different diameter were used. Three diameters were considered: 100 mm, 141 mm, and 200 mm. The fuel used in this study was n-heptane (98%). n-Heptane physical properties are shown in Table 1. The initial thickness of the fuel layer was maintained around 13 mm for each test. The freeboard length was initially 27 mm and increased as the fuel surface dropped. A total of 12 tests were conducted. Table 2 reports the characteristics of the different tests along with some of the measured quantities.

A top-loading balance was positioned below the tray to measure the fuel mass loss. Its range covered from 0 g to 6200 g with an accuracy of 0.01 g. To prevent heat transfer from the vessel to the balance, two 20 mm thickness insulators were placed between the vessel and the balance, as shown schematically in Fig. 1.

The effects of different initial temperatures on burning rates of n-heptane fires were studied with vessel filled with fuel placed on a heater and preheated to the sought temperature before the start of the test. The vessel was then moved on the insulators. The initial fuel temperatures were set between the ambient temperature and the fuel boiling point: 290 K, 319 K, 343 K, and 365 K.

The temperatures profiles in the fuel during the combustion were measured with 0.5 mm diameter K-type thermocouples. Nine thermocouples were arranged in the vertical axis of the vessel. Thermocouples were located at 1 mm, 2 mm, 3.5 mm, 5 mm, 6.5 mm, 8 mm, 10 mm, 11 mm, and 12 mm above the vessel bottom and are denominated TC1–TC9, as shown in Fig. 2. The temperature gradient at the wall surface in the direction of the vessel axis was also measured using thermocouples firmly built into the wall. Four thermocouples were placed on the inside of wall, named TC10–TC13, at heights of 2 mm, 6.5 mm, 12 mm and 27 mm from the bottom, respectively. The outputs of these sensors were recorded by a data acquisition system.

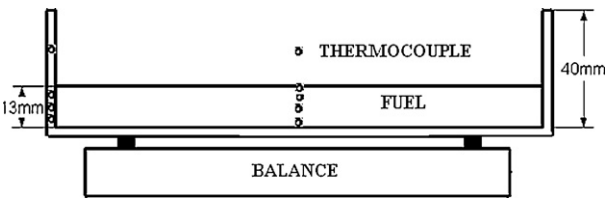

Fig. 1. Schematic diagram of the apparatus.

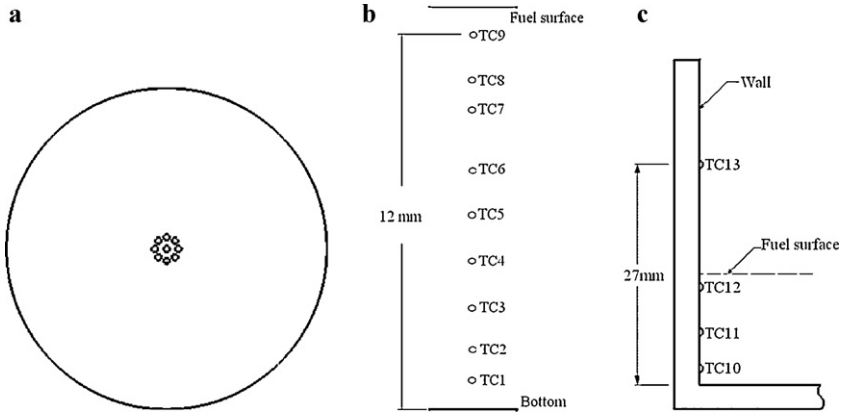

Fig. 2. Distribution of the thermocouples: (a) top view; (b) location of thermocouples; (c) vessel wall.

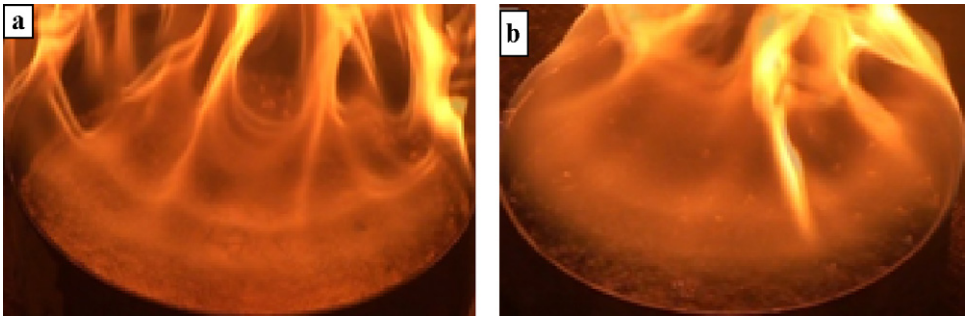

Fig. 3. Distribution of bubbles in fuel -for the 200 mm pool fire: (a) $T_{f,0}$ = 290 K; (b) $T_{f,0}$ = 365 K.

3. Results and discussion

3.1. Burning behavior of the pool fire

After ignition, fire rapidly spread until it became developed in the whole pool and reached a steady state regime for a certain period of time. A sharp increase of the flame height was then observed until a second steady regime was reached. The fire then decreased until it reached extinction due to burn out of fuel. The liquid fuel in the vessel was also observed during the experiments. For the cases under lower initial fuel temperature, during the initial development stage, the fuel remained unaffected and calm. After a quiet steady burning stage following initial stage, bubbles started to appear near the vessel wall and they eventually rose to the fuel surface. As the combustion evolved, more and more bubbles were observed in the entire liquid, as shown in Fig. 3a. These modes of burning can be defined: (1) unsteady following ignition, (2) steady burning with surface boiling, (3) transition to bulk boiling, (4) steady burning at bulk boiling, and (5) decrease to extinction. However, as observed in the experiments, the bubbles appeared more quickly and in greater amount and size when the initial fuel temperature was raised. For the case of initial fuel temperature of 365 K, large bubbles could be seen shortly after ignition (see Fig. 3b). The quiet steady burning, which appeared in lower initial temperature case, was not found.

The variation of fuel mass during combustion was obtained using the balance and then converted into mass burning rate. For the tests under different initial fuel temperature, two typical burn-

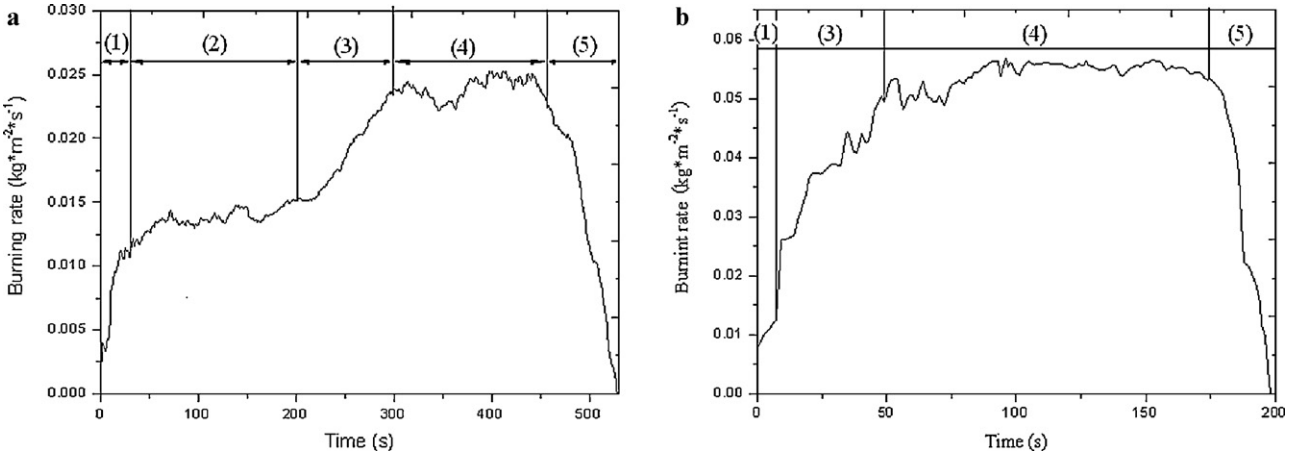

Fig. 4. Temporal evolution of n-heptane pool fire burning rate of same diameter D = 200 mm, but different initial temperature: (a) $T_{f,0}$ = 290 K; (b) $T_{f,0}$ = 365 K.

ing rate histories were observed. Fig. 4a shows the history of mass burning rate in a 200 mm pool fire with an initial fuel temperature of 290 K. Five possible stages can be identified:

(1) Initial development stage, corresponding to the fire development in the vessel. In this stage, fire size and burning rate increase. The duration of this stage depends on various parameters, such as vessel diameter and fuel type [21]. In our tests, this stage lasted about 20–30 s.
(2) Steady burning stage, corresponding to the developed fire that follows the initial development stage. In this stage, surface boiling starts to appear, and the burning rate during this stage is nearly constant.
(3) Transition stage, corresponding to a sudden increase of the burning rate. Big bubbles start to appear near the vessel wall and rise to the fuel surface.
(4) Bulk boiling burning stage, corresponding to the entire boiling fuel and fully developed fire, while bubbles could be found everywhere in the fuel. The burning rate in this stage is about two or more times that of steady burning stage.
(5) Decay stage, corresponding to end of the combustion. In this period, both of the fire size and burning rate decreases and finally extinguishes due to the burnout of fuel.

This burning process is similar to the one reported in Ref. [5], which considered a 50.5 mm of diameter n-heptane pool with an 11 mm depth. However, in present study, some different kinds of phenomenon are observed. From Fig. 4b, it can be seen that the steady burning stage (the second stage), disappears when the initial fuel temperature is 365 K. Transition process occurs following the initial development stage.These two burning rate histories obtained in present study are different from previous work, which was reported in Refs. [21,22]. In their research, only three stages have been observed: initial development, steady burning, and decay. The possible reason for this difference in burning process will be discussed below.

3.2. Burning rates of fires with increased initial fuel temperatures

Four different initial fuel temperatures, i.e. $T_{f,0}$ = 290 K, 319 K, 343 K, 365 K, were considered in n-heptane pool fires. Experimental results are summarized in Table 2. Note here $\dot{m}''_a$ denotes the time-average burning rate per area unit for the whole test duration, defined as the average value of burning rate for the total burning time. The mass burning rates $\dot{m}''_2$ and $\dot{m}''_4$ are the burning rates per area unit for steady burning stage (2), and bulk boiling burning stage (4), respectively. Fig. 5 presents the burning rates of 100 mm pool fires with different initial fuel temperatures.

For the 100 mm diameter pool, the case with an initial fuel temperature of $T_{f,0}$ = 290 K presents a steady burning rate $\dot{m}''_2$ of 0.0073 kg m^{-2} s^{-1}. Cases with initial fuel temperature of 319 K and 343 K present nearly similar steady burning rates $\dot{m}''_2$: 0.0074 kg m^{-2} s^{-1} and 0.0076 kg m^{-2} s^{-1}, respectively. The steady burning rates, $\dot{m}''_2$, are about 0.013 kg m^{-2} s^{-1} and 0.015 kg m^{-2} s^{-1} for the 141 mm and 200 mm pool fires for the different initial fuel temperatures considered in this study and does not vary significantly with increased initial fuel temperature. This indicates that for a given pan size and fuel thickness, the steady burning rate is independent of the initial fuel temperature. However, the decrease of the second stage duration under different initial temperature can be seen in Fig. 5 and Table 1. The duration is reduced from 210 s ($T_{f,0}$ = 290 K) to 92 s ($T_{f,0}$ = 343 K) for 100 mm pool fires. As mentioned above, the steady burning stage almost disappears for the case of 365 K. Thus it is believed that the duration of steady burning stage is shortened with increasing initial fuel temperature and becomes zero when the initial fuel temperature approaches the boiling point of the fuel used.

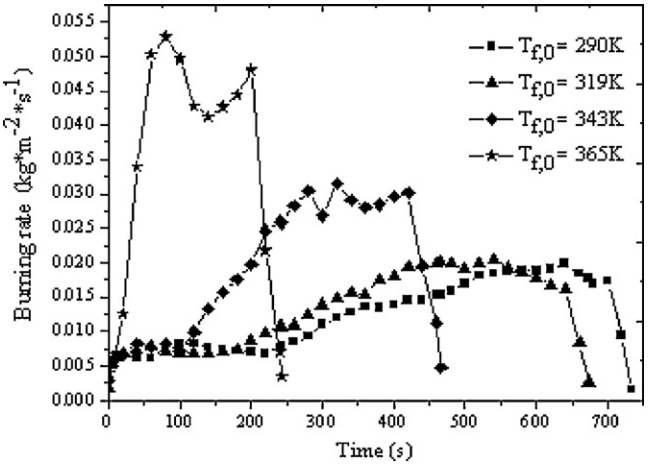

Fig. 5. Burning rates for the 100 mm heptanes pool fires.

The value of burning rate during the stage (4), $\dot{m}''_4$, increases with the increase of initial fuel temperature, as shown in Fig. 5. For the initial temperatures of 290 K and 365 K, the burning rate increases from 0.018 kg m^{-2} s^{-1} to 0.046 kg m^{-2} s^{-1}. The phenomenon that the burning rate depends on the initial fuel temperature is also observed in the 141 mm and 200 mm pool fires, (see Table 2). Moreover, the burning rate during the bulk boiling stage increases more than twice when the initial fuel temperature is elevated from 290 K to 365 K.

Table 2 shows the burning rate during the stage (4) increases significantly from the value of stage 2. The Burning Rate Ratio, BRR for short, is defined as the ratio of the bulk boiling burning rate observed in stage (4) over the steady burning rate observed in stage (2). The BRR for various dimensionless initial fuel temperatures are plotted in Fig. 6. In this figure, $T_{f,0}$ is the initial fuel temperature, $T_{f,b}$ is the fuel boiling point, and T_a is the ambient temperature. For an initial fuel temperature of 365 K, the steady burning rates of pool fires are assumed to equal the values those change slightly in the same diameter. The value in the previous study [5] is also plot in Fig. 6.

BRR shows the difference of the burning rate between the steady burning stage and bulk boiling burning stage. A similar ratio was introduced by Hayasaka [5] to model the influence of the fuel

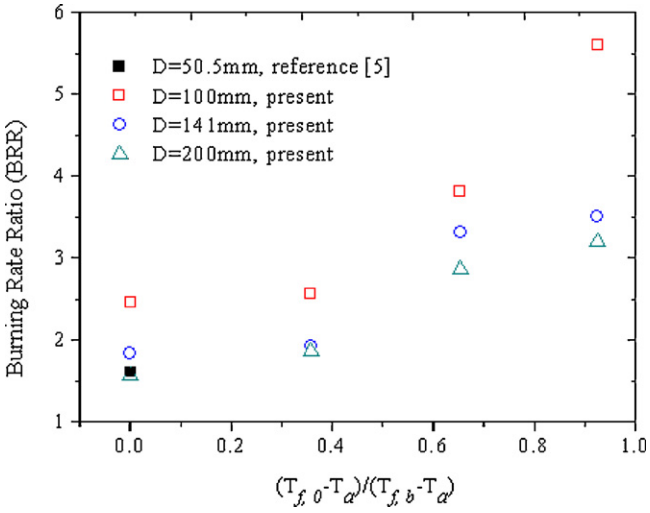

Fig. 6. Relation of the burning rate ratio and dimensionless initial fuel temperature.

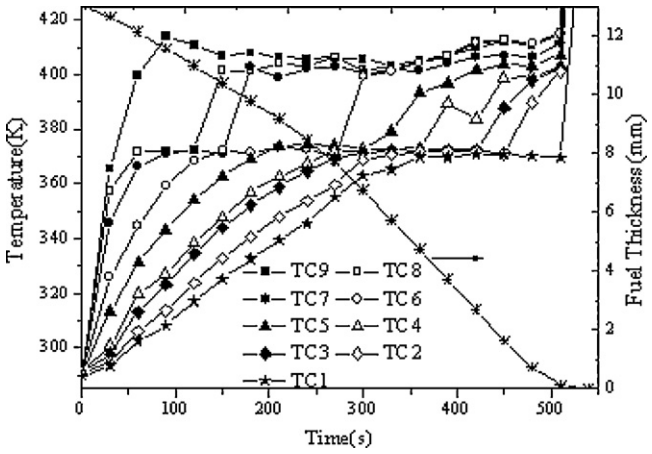

Fig. 7. Temporal evolutions of temperature at different locations and fuel thickness. D = 200 mm, $T_{f,0}$ = 290 K.

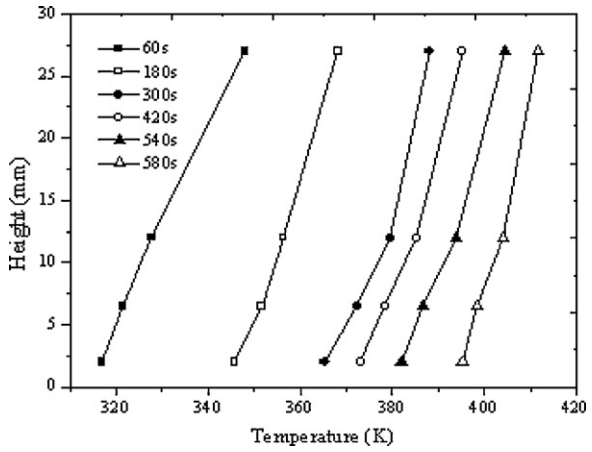

Fig. 8. Vertical temperature distribution of the vessel wall, D = 200 mm, $T_{f,0}$ = 290 K.

chemical complexity on the BRR. In his research, the initial fuel temperature was equal to the ambient temperature, and the difference in temperature between initial temperature and the boiling point of fuel was considered to calculate BRR. While it showed a clear increase of the BRR with an increase of the number of carbon atom in the fuel composition, the empirical equation also showed that the BRR decreased with the increase of the fuel initial temperature. However, from Fig. 6, BRR tends to become large when the initial fuel temperature increases, because of the increasing of burning rate in the stage 4. Thus, the relationship between BRR and parameters, such as the fuel type and initial fuel temperature, should be studied in detail in the future.

3.3. Temperature profiles in fuel and vessel wall

The temporal evolution of the fuel thickness, for the case involving a pool diameter of 200 mm with an initial temperature of 290 K is plotted in Fig. 7. The fuel mass temporal evolution was measured using a scale balance. From the knowledge of the remaining fuel mass, the fuel depth can be obtained as a function of time using the liquid fuel density. Since the fuel was not replenished during the test, the fuel thickness decreased and became zero at about 520 s.

The temperature distribution in the fuel was checked by nine thermocouples, from 1 mm (TC1) to 12 mm above the vessel bottom (TC9). Note that since the fuel thickness is 13 mm at ignition, TC9 is located just 1 mm below the surface of fuel. The values shown in Fig. 7 are temperature profiles across the fuel bed for the 200 mm-diameter fire test with an initial fuel temperature of 290 K. The profiles of temperature below the fuel surface show that the bulk fuel temperature increases after ignition. There is no distinguished cold zone formed in the liquid fuel during the fire. This result indicates that the assumption from the previous studies [17,23], the formation of a cold zone in the liquid, is not observed in this study. Under the vaporizing layer, there is a preheating layer formed after ignition where fuel temperature increases with time.

The temperature measured by TC9 shows that the fuel at 12 mm height reaches its boiling point (about 371 K) at about 30 s after ignition. Then the temperature keeps increasing to reach 410 K and almost remains constant for the remaining duration until the flame reaches the thermocouple at the end of the experiment, around 520 s. The other thermocouples exhibit a slightly different behavior. After an initial temperature raise more or less pronounced depending on the depth of the thermocouple, the temperature reaches the boiling point of the fuel used and plateaus until the fuel surface moves below the thermocouple. Then the temperature sharply increases to a nearly temperature of about 400–415 K and then remains constant until the final sharp increase at the flame burnout. It is interesting to note that once above the fuel surface, the thermocouples recorded nearly the same temperature. This temperature is recognized as the temperature of the hot gases above the fuel surface. The temperature gradient appears and the maximum temperature difference is only 10 K due to the relatively short distance (~10 mm). The dramatic temperature increase after 520 s is due to the effect of flame approaching the pan bottom when the fuel burnt out.

It is found that the fuel temperature reaches its boiling point before the fuel surface drops to that position. For example, the temperature of fuel at 6.5 mm height, measured by TC5, reaches boiling temperature at 200 s, while the fuel surface is about 9 mm height. This result shows that there is a boiling zone formed in the fuel, and the boiling zone thickness is about 2.5 mm at this time. Moreover, this zone gradually becomes big and finally reaches about 3.5 mm. This conclusion can be drawn from the fact that the fuel at 1 mm height from the bottom reaches the boiling point 350 s after ignition. Meanwhile, the fuel thickness is about 4.5 mm.

The temperature distribution at the wall surface was measured by four thermocouples. Fig. 8 shows the temperature profiles of 200 mm pool fire with an initial fuel temperature of 290 K. Temperature decreases from the top of the vessel to the bottom and the temperature difference between the top and bottom of wall becomes small with time. The vertical temperature gradient varies from 124 K/m to 45 K/m in this case.

3.4. The relation between burning rate and fuel temperature

A comparative analysis of the burning rate history and the fuel temperature curve will perhaps provide us with a better sense of the relation between them. For the case of 200 mm fire with an initial temperature of 290 K, Fig. 7 shows the fuel temperature increases with time and the fuel surface temperature is equal to its boiling temperature after the early 30 s. Then the bulk fuel completely reaches the boiling point at about 350 s. From Fig. 4a, we can see that the steady burning stage and Bulk boiling burning stage starts around these two times, respectively. A similar result was observed in Hayasaka's research [5]: boiling process started when the fuel temperature measured by one thermocouple at 1 mm height from bottom almost equaled the boiling point. This result indicates that the steady burning stage occurs when the fuel surface reaches the boiling point of the fuel used, while the stage 4, bulk boiling burning stage, starts at the time of occurrence of bulk fuel boiling.

As mentioned in Section 3.2, the duration of steady burning stage decreases with initial fuel temperature and almost disap-

pears in the case with the initial temperature of 365 K, Based on the discussion above, this result can be explained as follows: for a given amount of liquid fuel, less heat flux is needed to heat fuel to the boiling point and the bulk boiling phenomena occurs much quicker if the fuel has a higher temperature. Similarly, the bulk boiling burning stage would not occur if the bulk fuel could not reach its boiling temperature. Hence, in the cases with semi-infinite liquid, only three stages, initial development, steady burning, and decay, are expected.

Moreover, as the initial temperature increased, little fuel is consumed during the steady burning stage, and more fuel remains in the vessel when the bulk liquid boiling occurs. In this situation, the boiling becomes more violent, as observed in the tests. It is believable that more and bigger bubbles in the liquid would enhance the heat exchange, resulting in the increasing of burning rate.

4. Conclusion

An experimental study of n-heptane pool fires was conducted considering different initial fuel temperatures for three different diameter trays. Temperature distributions in fuel and vessel wall, and burning rate were measured during the test. The major conclusions are summarized below:

(1) Five possible stages were identified: initial development stage, steady burning stage, transition stage, bulk boiling burning stage and decay stage. Experimental results show that the duration of steady burning stage decreases with the initial fuel temperature and would become zero when the initial temperature approaches the boiling point of fuel used.
(2) For a given pool diameter, the burning rate in the steady burning stage is constant regardless of the initial fuel temperature. However, its value increases during the bulk boiling stage, with more intensity as the increased initial fuel temperature is high. The bulk boiling burning rate, $\dot{m}''_4$, has been observed to be twice or more greater than the steady burning stage burning rate, $\dot{m}''_2$.
(3) The fuel surface temperature increases rapidly after ignition and remains equal to its boiling point during the combustion. Vertical temperature gradient in the liquid is observed after ignition, but bulk temperature becomes almost uniform in the latter stages. Boiling zone is formed and its thickness becomes bigger with time until bulk boiling occurs.
(4) Steady burning stage starts at the time that the fuel surface temperature equals the boiling point; while bulk boiling burning stage occurs when the bulk liquid fuel reaches boiling temperature.

Acknowledgments

This work was sponsored by National Natural Science Foundation of China with Projects no. 51036007 and no. 50976109 and by the CAS Special Grant for Postgraduate Research, Innovation and Practice. The authors also thank Prof. James. G. Quintiere for his help with the discussion.

References

[1] E. Planas–Cuchi, H. Montiel, J. Casal, A survey of the origin, type and consequences of fire accidents in process plants and in the transportation of hazardous materials, Trans. IchemE. 75 (1997) 3–8.
[2] V.I. Blinov, G.N. Khudiakov, Certain laws governing diffusive burning of liquids, Academmiia Nauk, SSSR Doklady 113 (1957) 1094–1098.
[3] I.V. Blinov, G.N. Khudiakov, Diffusive burning of liquids, Report No. T-1490a-c, ASTIA, AD296762, US Army Engineering and Research Laboratories, 1961.
[4] D. Burgess, A. Strasser, J. Grumer, Division of Fuel Chemistry American Chemical Society, Symposium on Fire Control Research, Chicago, Illinois, 1961, pp. 177–192.
[5] H. Hayasaka, Unsteady burning rates of small pool fires, in: Proc.5th Symp. (Int.) on Fire Safety Sci., Melbourne, 1997, pp. 499–510.
[6] V.B. Apter, A.R. Green, J.H. Kent, Pool Fire Plume Flow in a Large-scale Wind Tunnel, in: Proc. 3rd Symp. (Int.) on Fire Safety Sci., London, 1991, pp. 425–434.
[7] Hiroshi Koseki, G.W. Mulholland, The effect of diameter on the burning of crude oil pool fires, Fire Technol. 27 (1) (1991) 54–65.
[8] J.L. Torero, S.M. Olenick, J.P. Garo, J.P. Vantelon, Determination of the burning characteristics of a slick of oil on water, Spill Sci. Technol. Bull. 8 (2003) 379–390.
[9] F.M. Ferrero, B. Kozanoglu, J. Casal, J. Arnaldos, Experimental study of thin-layer boilover in large-scale pool fires, J. Hazard. Mater. 137 (2006) 1293–1302.
[10] J. Fang, C.Y. Yu, R. Tu, The influence of low atmospheric pressure on carbon monoxide of n-heptane pool fires, J. Hazard. Mater. 154 (2008) 476–483.
[11] Z.H. Li, Y.P. He, H. Zhang, J. Wang, Combustion characteristics of n-heptane and wood crib fires at different altitudes, Proc. Combust. Inst. 32 (2009) 2481–2488.
[12] L.H. Hu, S. Liu, W. Peng, R. Huo, Experimental study on burning rates of square/rectangular gasoline and methanol pool fires under longitudinal air flow in a wind tunnel, J. Hazard. Mater. 169 (2009) 972–979.
[13] J.S. Roh, S.S. Yang, H.S. Ryou, Tunnel fires: experiments on critical velocity and burning rate in pool fire during longitudinal ventilation, J. Fire Sci. 25 (2007) 161–176.
[14] Y. Utiskula, J.G. Quintiere, A.S. Rangwala, B.A. Ringwelski, K. Wakatsuki, T. Naruse, Compartment fire phenomena under limited ventilation, Fire Safety J. 40 (2005) 367–390.
[15] A. Hamins, J. Yang, T. Kashiwagi, A Global model for predicting the burning rates of liquid pool fires, Report No. NISTIR 6381, US Department of Commerce, 1999.
[16] A. Nakakuki, Heat transfer in small scale pool fires, Combust. Flame 96 (1994) 311–324.
[17] A. Nakakuki, Heat transfer in hot-zone-forming pool fires, Combust. Flame 109 (1997) 353–369.
[18] M. Muñoz, J. Arnaldos, J. Casal, E. Planas, Analysis of the geometric and radiative characteristics of hydrocarbon pool fires, Combust. Flame 139 (2004) 263–277.
[19] M. Muñoz, E. Planas, F. Ferrero, J. Casal, Predicting the emissive power of hydrocarbon pool fires, J. Hazard. Mater. 144 (2007) 725–729.
[20] J.A. Fay, Model of large pool fires, J. Hazard. Mater. 136 (2006) 219–232.
[21] J.M. Chatris, J. Quintela, J. Folch, E. Planas, J. Arnaldos, J. Casal, Experimental study of burning rate in hydrocarbon pool fires, Combust. Flame 126 (2001) 1373–1383.
[22] J.G. Quintiere, Fundamentals of Fire Phenomena, Wiley, West Sussex, 2006.
[23] A. Nakakuki, Heat transfer in pool fires at a certain small lip height, Combust. Flame 131 (2002) 259–272.